Electronic Supplementary Information (ESI) for:

Encapsulation of 3D Plasmonic Nanostructures with Hydrogel Skin for Rapid and Direct Detection of Toxic Small Molecules in Complex Fluids

Sunho Kim[†a], Wook Choi[†b], Dong Jae Kim[a], Ho Sang Jung[b], Dong-Ho Kim[b], Shin-Hyun Kim[*a] and Sung-Gyu Park[*b]

[a]Department of Chemical and Biomolecular Engineering (BK21+ Program) KAIST, Daejeon, 34141 Korea

[b]Advanced Nano-Surface Department, Korea Institute of Materials Science (KIMS), Changwon, Gyeongnam 641-831, Korea Phone: +82-55-280-3632 Fax: +82-55-280-3570 E-mail: sgpark@kims.re.kr

[†]These authors contributed equally to this work.

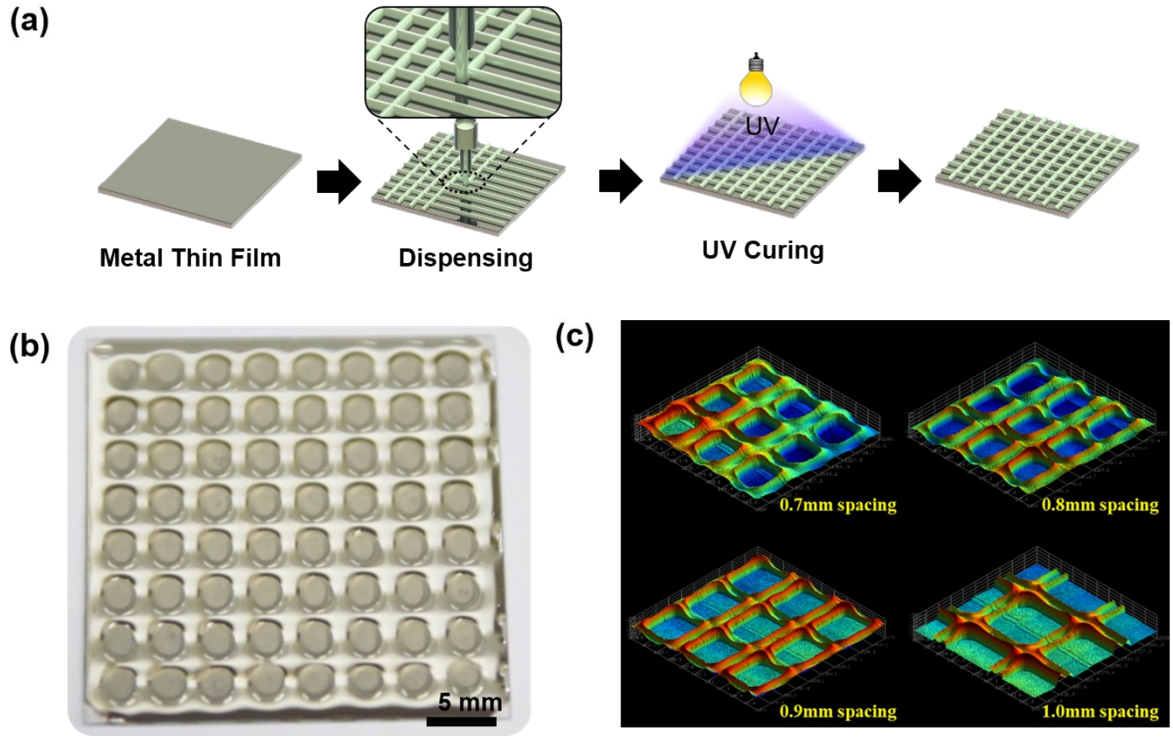

Fig. S1 (a) Schematic illustration for the fabrication of multiple microwells on a single substrate. (b) Image of the microwell array. (c) 3D topologies of microwell arrays with four different spacings obtained by a confocal microscope.

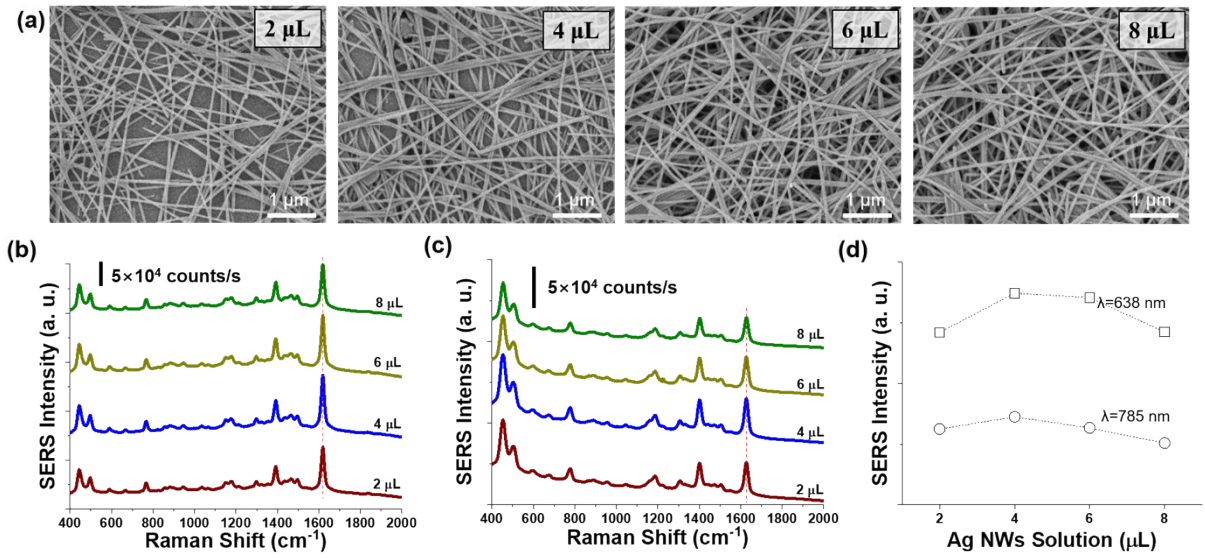

Fig. S2 (a) SEM images of the 3D multiple stacks of AgNWs prepared by depositing four different volumes of AgNW suspensions: 2 μL, 4 μL, 6 μL, and 8 μL. (b, c) Raman spectra of methylene blue (MB) measured from the multiple stacks in (a) on which 2 μL aqueous solution of MB at the concentration of 5×10^{-6} M is deposited and dried, where lasers with wavelengths of 638 nm (b) and 785 nm (c) are respectively used. (d) Raman intensity at the Raman shift of 1628 cm^{-1} as a function of the volume of AgNW suspension for two different wavelengths of lasers.

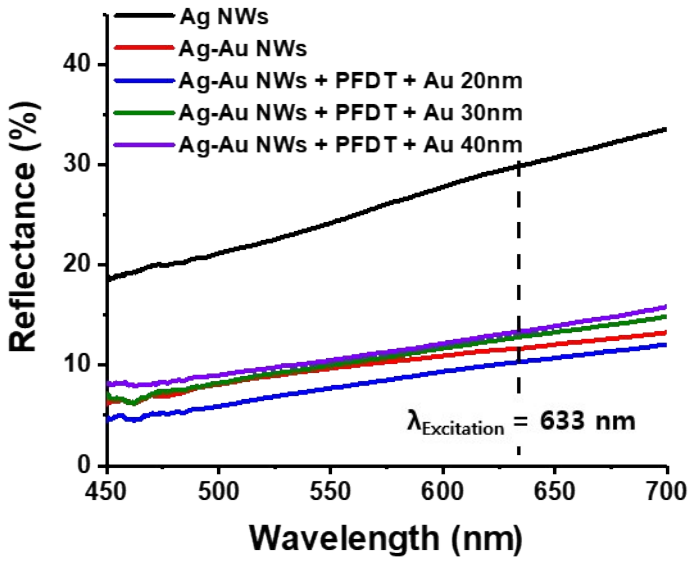

Fig. S3. Reflectance spectra measured from the 3D multi-stacks of AgNWs, Ag-Au NWs, and Ag-Au NWs decorated with Ag NPs of three different deposition conditions.

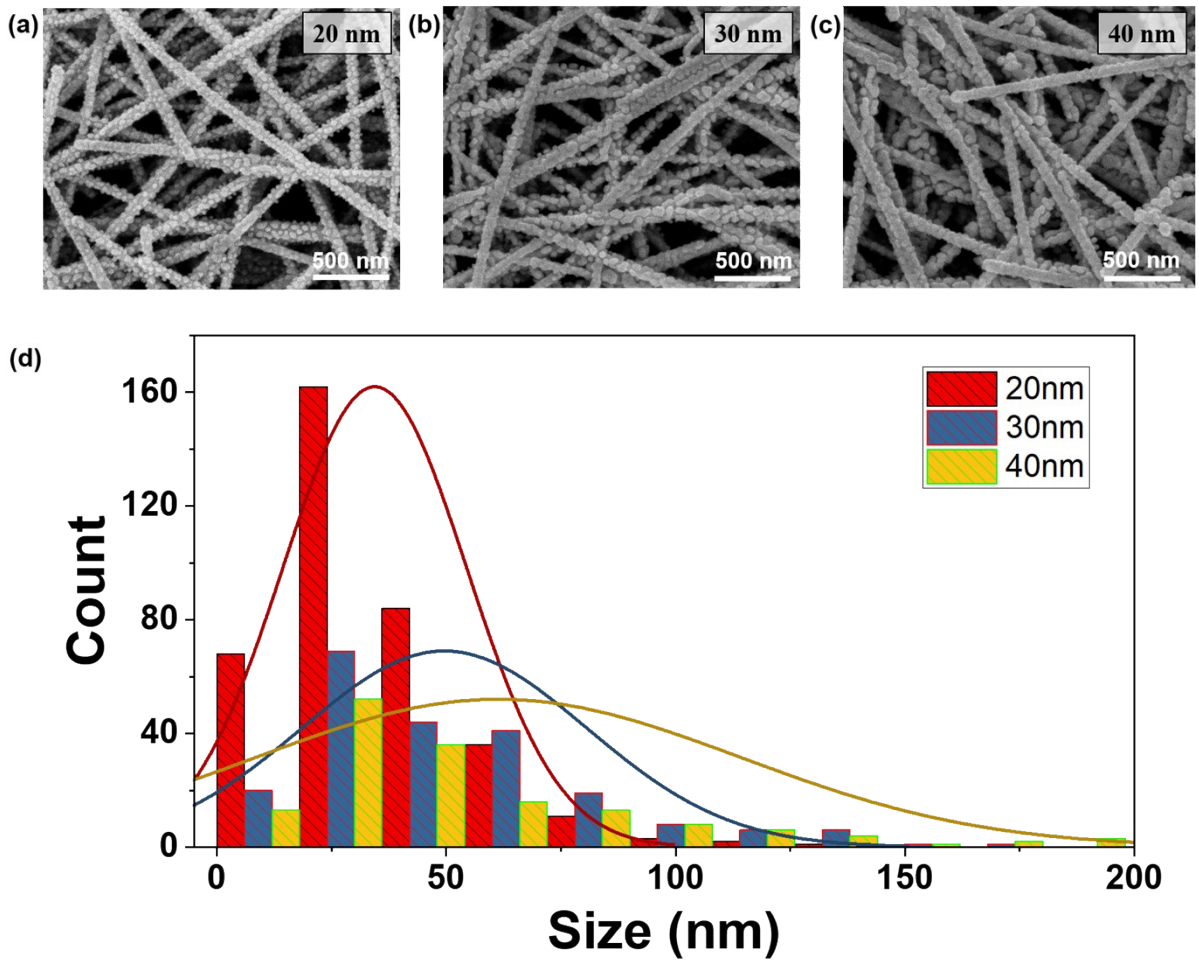

Fig. S4 (a-c) SEM images of hierarchical nanostructures composed of multi-stacked Au-Ag NWs whose surfaces are decorated with Ag NPs, where Ag deposition conditions by which (a) 20-nm-, (b) 30-nm-, and (c) 40-nm-thick layer are formed on a flat surface are used. (d) Histogram of the size distribution of spherical Ag NPs deposited on Au–Ag NWs for the three different deposition conditions. The solid lines are fitting curves with the Gaussian equation

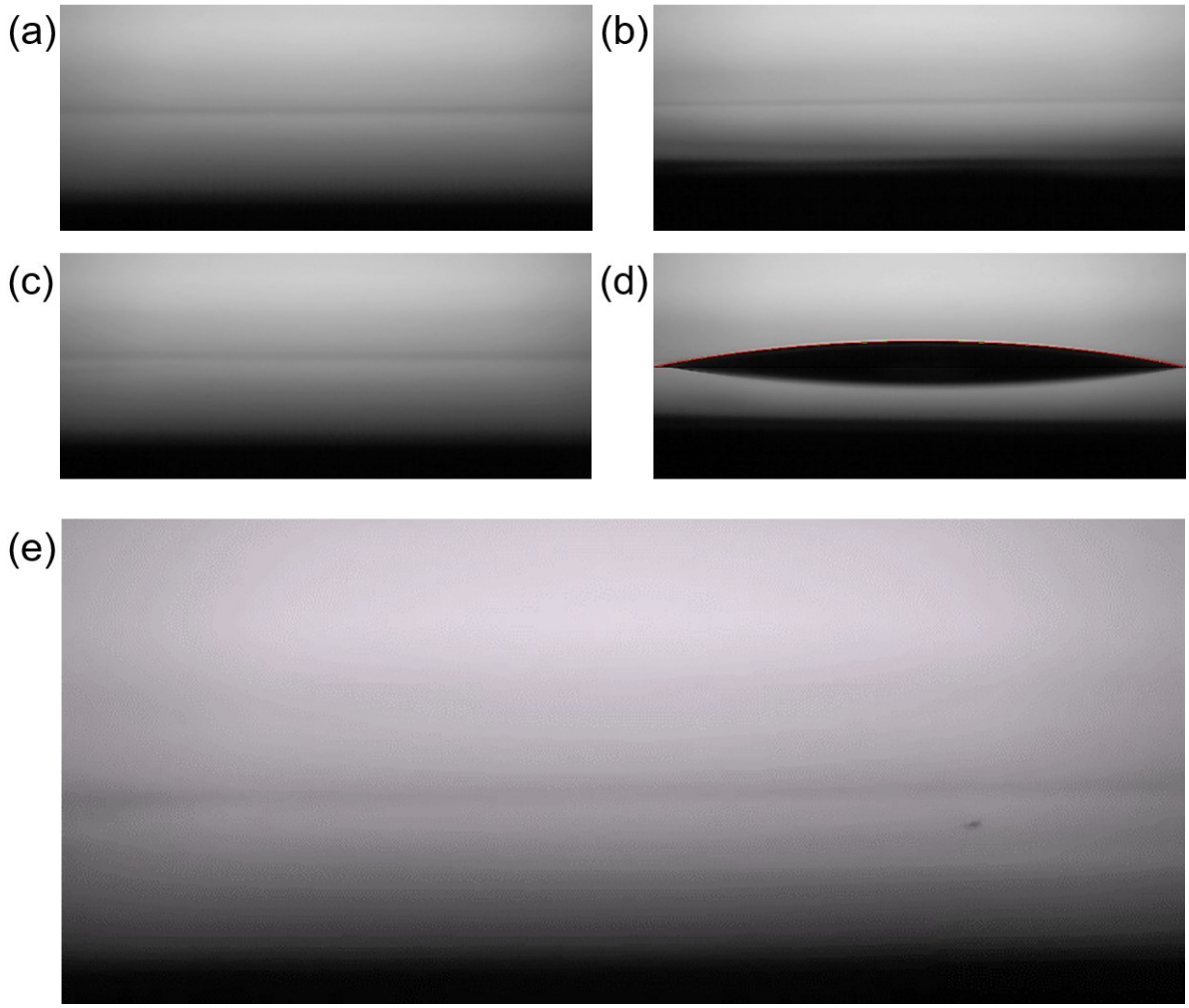

Fig. S5. (a-d) Images showing wetting state and contact angle of ethanolic solutions containing PEGDA and water, where 3 μL of the solutions are deposited on Ag-deposited PEN film: (a) 1.4 w/w% PEGDA, 0.6 w/w% water, and 98.0 w/w% ethanol, (b) 7.0 w/w% PEGDA, 3.0 w/w% water, and 90.0 w/w% ethanol, (c) 14.0 w/w% PEGDA, 6.0 w/w% water, and 80.0 w/w% ethanol, and (d) 35.0 w/w% PEGDA, 15.0 w/w% water, and 50.0 w/w% ethanol. The solutions with compositions of (a-c) show total wetting and that of (d) shows the contact angle of 12°. (e) Time series of images showing wetting state for the solution of 7.0 w/w% PEGDA, 3.0 w/w% water, and 90.0 w/w% ethanol. The ethanol is fully depleted at 42 s. There is no transition from total wetting to partial wetting.

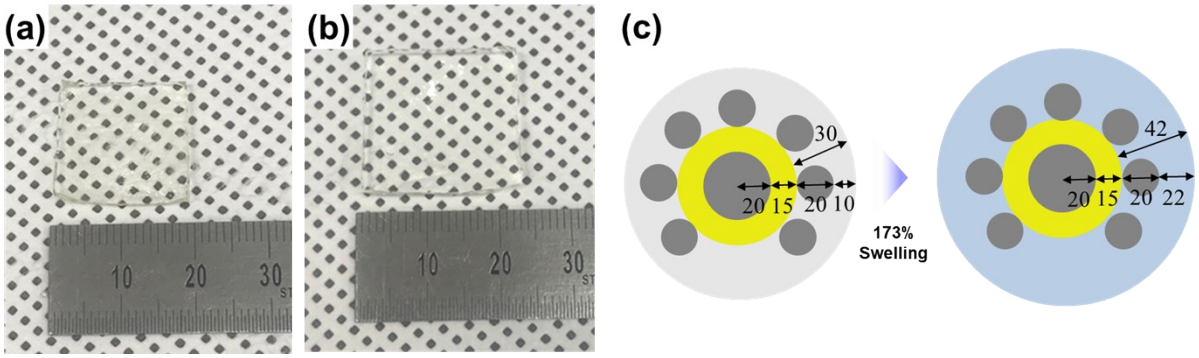

Fig. S6. (a, b) Photographs of a bulk hydrogel film in the air (dried state, a) and water (wet state, b). The film is prepared using a mixture of 69.6 w/w% PEGDA and 29.9 w/w% water, and 0.5 w/w% photoinitiator and immersed in distilled water for 10 hours for the wet state. The lateral dimension of the square-shaped film is 2.0 cm at the dried state, which increases to 2.4 cm in the wet state. (c) Simplified models of the cross-sections of ultrathin-hydrogel-encapsulated Ag-Au NWs decorated with Ag NPs. Dimensions are denoted in the image with a unit of nm. Assuming that the initial volume fraction of Ag NPs embedded in cylindrical hydrogel skin is 20% and the hydrogel skin is swollen by 173% in volume, the average thickness of wet hydrogel skin is estimated as approximately 32 nm.

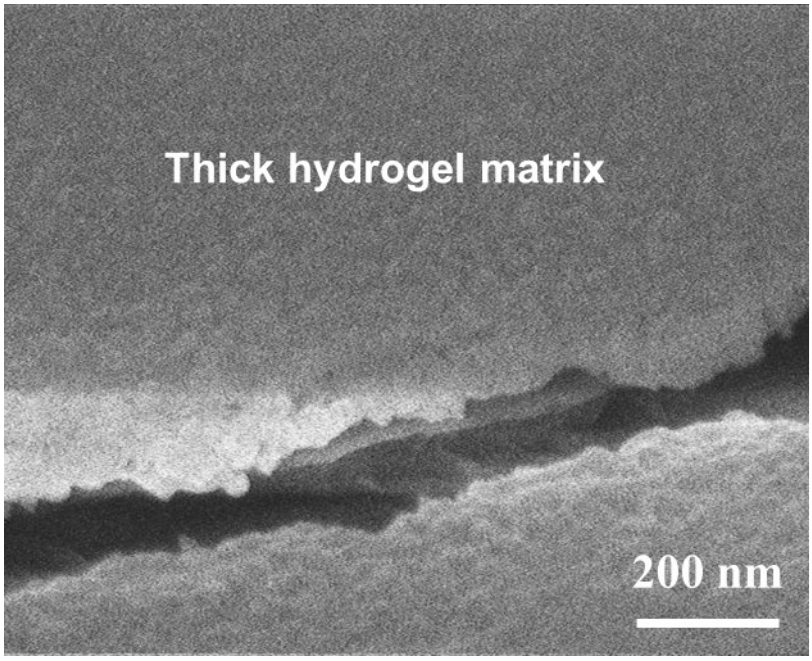

Fig. S7. SEM images of a thick-hydrogel-encapsulated nanostructure. The hydrogel occupies whole interstitial voids among NWs and overcoats the nanostructure.

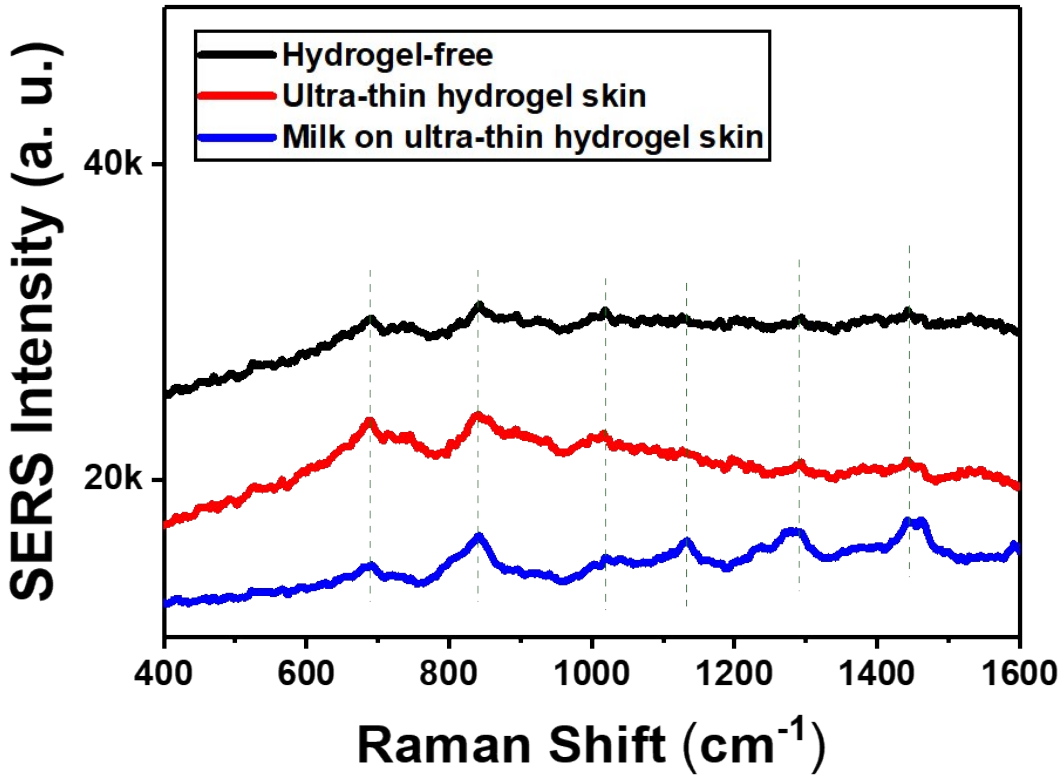

Fig. S8. Raman spectra obtained from the hydrogel-free nanostructure dipped in distilled water (black line), ultrathin hydrogel-encapsulated nanostructure dipped in distilled water (red line), and ultrathin hydrogel-encapsulated nanostructure dipped in milk (blue line). The vertical dotted lines indicate the common peaks for three spectra, which are originated from poly(vinylpyrrolidone) (PVP), the capping agent of Ag NWs.

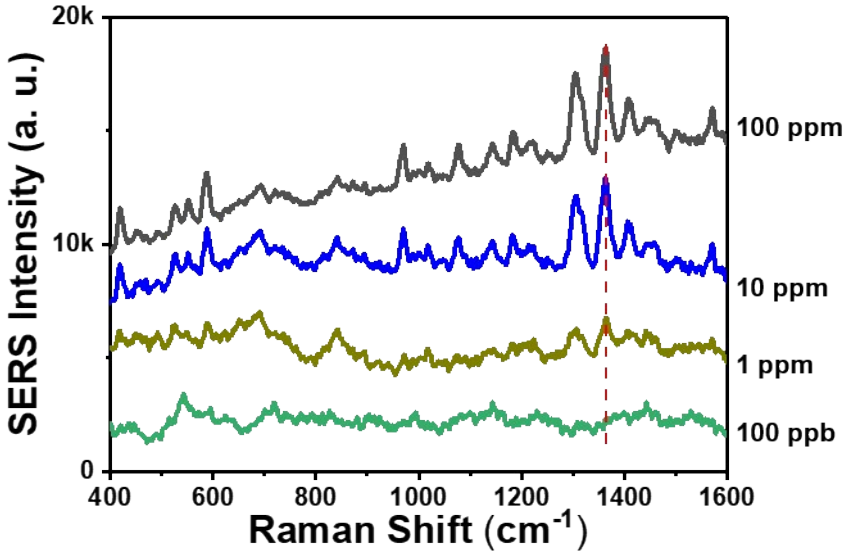

Fig. S9. Raman spectra of tricyclazole spiked in milk at various concentrations measured from the hydrogel-free bare nanostructure.

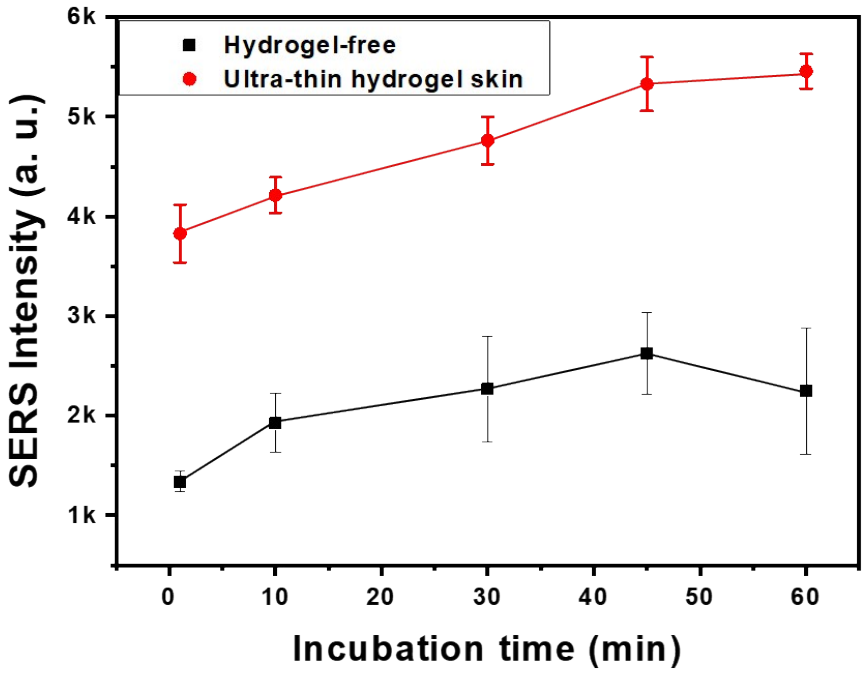

Fig. S10. Raman intensity at 1365 cm^{-1} as a function of incubation time of the hydrogel-free bare nanostructure (black squares) and the ultrathin-hydrogel-encapsulated nanostructure (red dots) in milk containing 1 ppm tricyclazole. The Raman spectra are acquired after complete drying. The error bars indicate the standard deviations for 5-times of measurement.

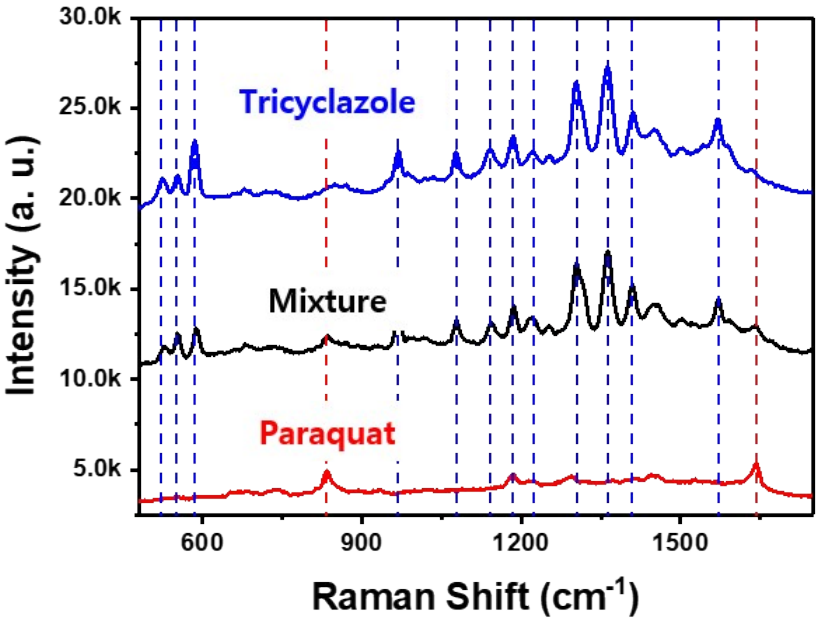

Fig. S11. Raman spectra, measured using the ultrathin-hydrogel-encapsulated nanostructures, of tricyclazole (blue curve), paraquat (red curve), and a mixture of tricyclazole and paraquat (black curve) that are respectively spiked in whole milk at the concentration of 1 ppm. Blue and red dotted lines indicate characteristic peak positions for tricyclazole and paraquat, respectively.